Evaluation of Positioning Algorithms for Wide Area Multilateration based Alternative Positioning Navigation and Timing (APNT) using 1090 MHz ADS-B Signals

Shau-Shiun Jan and Siang-Lin Jheng
Department of Aeronautics and Astronautics, National Cheng Kung University, Taiwan
Yu-Hsuan Chen and Sherman Lo
Department of Aeronautics and Astronautics, Stanford University, USA

BIOGRAPHY

Shau-Shiun Jan is an associate professor of the Department of Aeronautics and Astronautics at National Cheng Kung University (NCKU) in Taiwan. He directs the NCKU Communication and Navigation Systems Laboratory (CNSL). He received the Ph.D. in Aeronautics and Astronautics from Stanford University.

Siang-Lin Jheng received his B.S. degree in Aerospace Engineering at Tamkang University (TKU) in 2011. He received his M.S. degree in the Institute of Civil Aviation at NCKU in 2013. He is currently studying for his Ph.D. degree in the Department of Aeronautics and Astronautics at NCKU in Taiwan.

Yu-Hsuan Chen is a research associate at the Stanford GPS Laboratory. He received his Ph.D. in electrical engineering from NCKU, Taiwan. His research interests include real-time GNSS software receiver, antenna array processing and APNT.

Sherman Lo is currently a senior research engineer at the Stanford GPS Laboratory. He is the Associate Investigator for the Stanford University efforts on the FAA evaluation of alternative position navigation and timing (APNT) systems for aviation. He received the Ph.D. in Aeronautics and Astronautics from Stanford University.

ABSTRACT

GNSS is the major technology that supports the operation of the modern air traffic management (ATM) system. Also, the positioning performance of GNSS is enhanced by many augmentation systems by providing corrections to the error sources as well as the integrity messages on the post-correction error residuals. However, unpredictable factors on the ground user environment, such as the radio frequency interference (RFI) could severely degrade or interrupt the service of GNSS receivers. In order to maintain the normal operation of the ATM system during GNSS outages, the alternative position, navigation and timing (APNT) service is essential. One of the possible approaches to provide the APNT service is the use of existing ADS-B data link at 1090 MHz to perform wide area multilateration (WAM).

In consideration to use the existing ADS-B data link for APNT, the current ground based transceiver (GBT) network that is originally deployed for surveillance purpose could be used as the WAM station to measure the signal time-of-flight to estimate the time of arrival (TOA). The attractive part of this 1090 MHz ADS-B WAM approach is that there infrastructure to support reception of the signal is already or being installed. However, these stations generally do not guarantee precise (~ 50 nanoseconds) or GNSS interference robust time synchronization. Hence a challenging issue to meeting the navigation and surveillance requirements of APNT is developing an appropriate time synchronization scheme for the ground stations. In ION GNSS+ 2013 conference, we presented the post processing results of ADS-B WAM test beds as well as the time synchronization designs in order to get adequate ranging performance.

In this paper, we will first investigate the positioning algorithms for this approach, and the positioning algorithms under consideration are 1) the linear iterative least squares method, 2) the non-iterative quadratic equation solution method, and 3) a hybrid of the prior 2 methods. Also, the station geometry effects on the positioning algorithms (i.e., dilution of precision (DOP)) will be evaluated. In order to keep the time for extended period when GPS is outage, the filter design to model the clock will then be studied. That is, with the model of the clocks' characteristics we would be able to predict the clock behavior to continue the normal operation of our ADS-B WAM test bed.

1. INTRODUCTION

The Federal Aviation Administration (FAA) Next Generation Air Transportation System (NextGen) relies heavily on Global Navigation Satellite System (GNSS)

and Automatic Dependent Surveillance – Broadcast (ADS-B) to support improved Communication, Navigation, Surveillance, and Air Traffic Management (CNS/ATM). The use of GNSS is enhanced by many augmentation systems to support the modern ATM system. However, unpredictable factors in the user environment may severely degrade the signal quality and interrupt GNSS operations. For example, when GNSS signals are blocked by the intentional or unintentional interference and jamming, widespread disruption of position, navigation, and timing services resulting in degraded CNS/ATM operations may be encountered. In recent years, the FAA has engaged in developing an alternative positioning, navigation, and timing (APNT) service to maintain the efficient air traffic operations during GNSS outages, even in high density airspaces. In addition to supporting key navigation operations, APNT also seeks to support surveillance by providing positioning suitable for three-mile aircraft separation [4].

ADS-B operation has been implemented to provide improved surveillance capabilities with ADS-B equipped aircraft periodically broadcasts their position derived from GNSS. ADS-B provides high accuracy surveillance for air traffic control (ATC) as well as traffic awareness to nearby aircraft. ADS-B is key technology for providing APNT. The existing ADS-B ground infrastructure consists of about 660 Ground Based Transceivers (GBT) are over the Conterminous United States (CONUS). These ground stations are located Distance Measuring Equipment (DME) and ADS-B [5-6]. These ground stations receive ADS-B information and re-broadcast ADS information (ADS-R) as well as provide traffic information service-broadcast (TIS-B). The internationally adopted for ADS-B radio standards is Mode S Extended Squitter (ES) transmitted on 1090 MHz. Other signals are also being developed for ADS-B, such as 978 MHz Universal Access Transceiver (UAT). Because the Mode S ES ADS-B is widely adopt for most of commercial airplanes and the fact that it will be the major surveillance system in the NextGen, this work will investigates the performance of Mode S ES signal to provide APNT capabilities.

One of the APNT concepts proposed by FAA adopts passive Wide Area Multilateration (WAM) which utilizes the existing ADS-B ground station facility to measure the time of arrival of the ADS-B signals broadcasted from aircrafts, as illustrated in Figure 1. TOA measurements of the same signal at multiple stations allow for calculation of the position of the transmitting source. The TOA measurement yields a passive or “pseudo” range and the process of position calculation is similar to GNSS is termed multilateration (MLAT). ADS-B ground stations make excellent MLAT station as the periodic ADS-B transmissions from aircraft allows for regular determination the position of an aircraft [4].

WAM positioning based on the Differential Time of Arrival (DTOA) method requires: 1) fixed-location receivers and 2) precisely synchronized clocks. Highly accurate and precisely synchronized clocks in the fixed location receivers are thus the most important elements and challenging issue to meet the navigation and surveillance requirements of APNT. In [1-2], we have proposed a ADS-B WAM time synchronization design and access its performance using post-processing. Additionally previous work examined means of providing robust precise timing to support ranging and multilateration [3]. The next step is reasonably to investigate the positioning algorithms for the WAM, which is the goal of this paper.

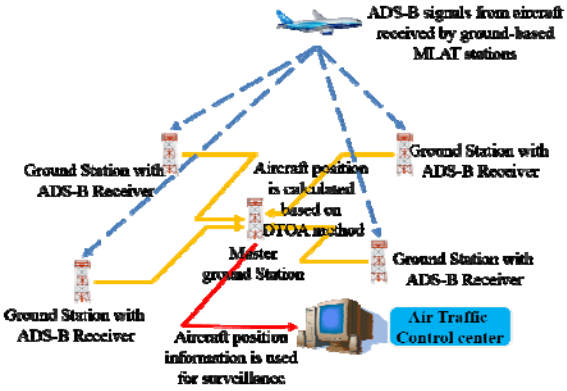

Figure 1: The working principle of the WAM system in a surveillance application.

The work in this paper focuses on the 1090 MHz signal, as 978 MHz UAT signal is not implemented in the Taipei Flight Information Region (FIR). The experimental MLAT ground station equipment was developed by using relatively low cost instruments. The 1090MHz ADS-B signals are collected by the universal software receiver peripheral (USRP). Each USRP is coupled with a GPS disciplined oscillator (GPSDO) to collect the raw data. GPSDO provides the 10 MHz synchronized clock for data sampling as well as the accurate 1 pulse per second (PPS) which can align the first sample with absolute time. This method can allow the geographically distributed USRP devices to use the same time reference and enables position determination using DTOA method. In this paper, we present two positioning methods and they are 1) the linear iterative least squares method, and 2) the non-iterative quadratic equation solution method. Additionally, the ground station distribution geometry effects on the positioning algorithms (i.e., dilution of precision (DOP)) will be evaluated in this paper as well.

Accordingly, the rest of the paper is organized as follows: Section 2 describes the interpolation method to improve the synchronization scheme proposed in [7]. Then, the means to obtain the 1090 MHz ranging signal measurements is explained, and WAM positioning algorithms are evaluated in Section 3. Also, the advantages of combination two different methods will be assessed in Section 4. Section 5 presents the experiment

setup and results. The final section presents the concluding remarks and the suggested future work.

2. TIME SYNCHROINZATION TEST BED

The most challenging issue to meet the navigation and surveillance requirements of APNT is the time synchronization scheme for the ground stations [5]. In [2], we presented post processing results of the ADS-B WAM test bed as well as the time synchronization designs to achieve adequate ranging performance. Two different clock standards, GPSDO and Rubidium clock, are presented here to evaluate the clock characteristic in order to operate an ADS-B WAM test bed. Figures 2 and 3 show the time synchronization test beds for the GPSDO and the Rubidium clock, respectively. The configurations of both figures are for the zero baseline tests. In Figure 2, two equipment sets share one common ADS-B antenna and ADS-B low noise amplifier (LNA). The two USRP based ADS-B receivers are synchronized by their respective onboard GPSDOs. The GPSDO acts as a stable oscillator and provides 1 pulse per second (PPS) for ADS-B receiver to synchronize the collection of data sampling. On the other hand, in Figure 3, Rubidium clock is used as the common clock for the test bed (using the 10 MHz input), and GPS receivers are employed to provide 1 PPS.

To evaluate the synchronization capabilities of the above test beds, one equipment set is regarded as the master station, and the other is regarded as the slave station. Then, the signal time of arrival (TOA) at the master station is t_1, and the signal TOA at the i^{th} slave station is t_i. The difference between each t_i and t_1 is defined as the differential time of arrival (DTOA) which is the key measurement for positioning. As a result, the DTOA can be expressed as

$$DTOA = (t_i - t_1), \tag{1}$$

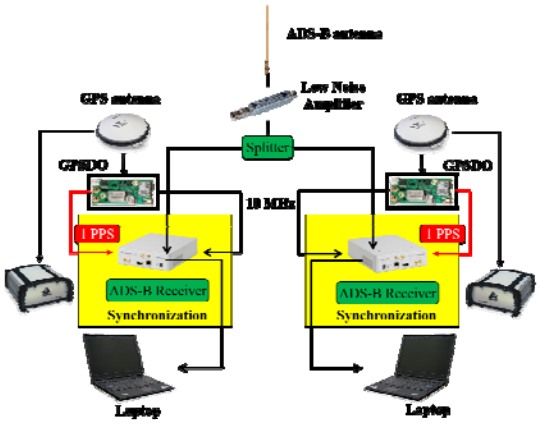

Figure 2: System configuration for zero baseline test with the GPSDO.

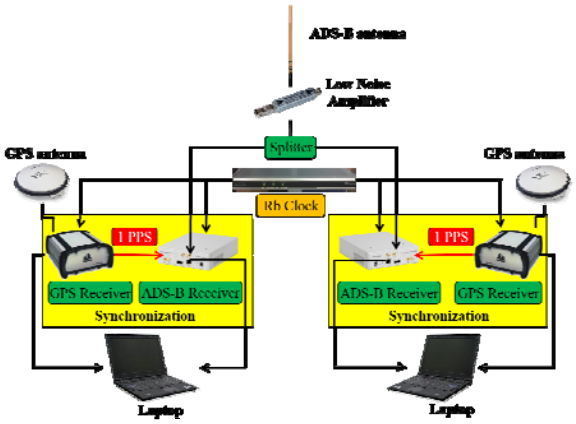

Figure 3: System configuration for zero baseline test with the Rubidium clock and GPS receiver.

The two equipment sets shown in Figures 2 and 3 share one common antenna, and the DTOA between these two should be zero ideally. However, due to some environmental uncertainties, as is shown later, the actual DTOA values are not zero. In experiments, we take 10 MHz sampling rate to collect the ADS-B data and we start all devices at the same time based using the 1 PPS from either GPSDO (Figure 2) or GPS receiver (Figure 3) as the trigger to start data collection. The 10 MHz is used to steer the clocks for the GPSDO and the Rubidium clock. This synchronizes the first sample. After the data collection, the cross-correlation technique is used to detect the TOA values. The cross-correlation technique is described in [7], and the calculation in the discrete time sampling is as follows:

$$C_{\max} = \frac{1}{N}\sum_{k=1}^{N} s_1(kT_s)\, s_2(kT_s + \tau). \tag{2}$$

where s_1 denotes the signal segment, s_2 denotes the signal segment with time delay τ, T_s is sampling interval, and N is number of samples. Additionally, the estimated correlation function can be approximated by a parabola in the nearby samples of its maximum as follows [7]:

$$C_{\max} = a\tau^2 + b\tau + c. \tag{3}$$

where a, b and c are fitting parameters to the cross-correlation result. The final time delay estimation D_τ can be calculated by Equation (4) [7].

$$D_\tau = -\frac{b}{2a} \tag{4}$$

The DTOA results of the zero baseline time synchronization tests for the GPSDO and the Rubidium clock are shown in Figure 4 and Figure 6, respectively. Figures 5 and 7 are the resulting histograms of the time differences (DTOAs). As shown in the figures, the standard deviation is 6.5 ns or equivalently 1.95 m when

using GPSDO clock, and the standard deviation is 14 ns or equivalently 4.2 m when using the Rubidium clock. Moreover, Figure 4 shows that GPSDO clock has a noticeable constant clock drift relative to each other. . These results are consistent with the specifications provided by the manufacturers, and they meet the requirements of APNT for the time synchronization accuracy of less than 50 ns [8].

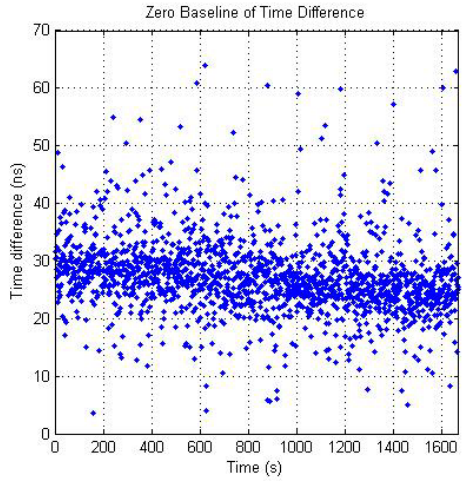

Figure 4: Time difference result for the zero baseline test with the GPSDO.

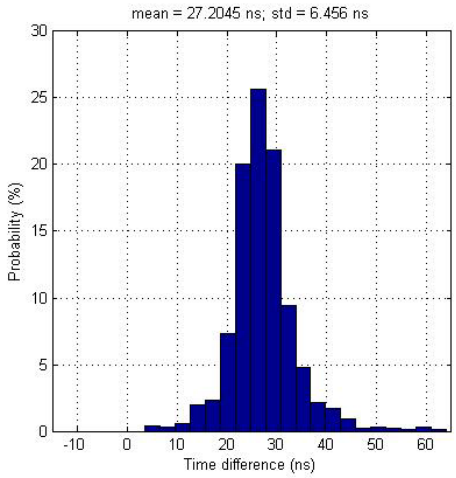

Figure 5: Histogram of time difference estimates for the GPSDO.

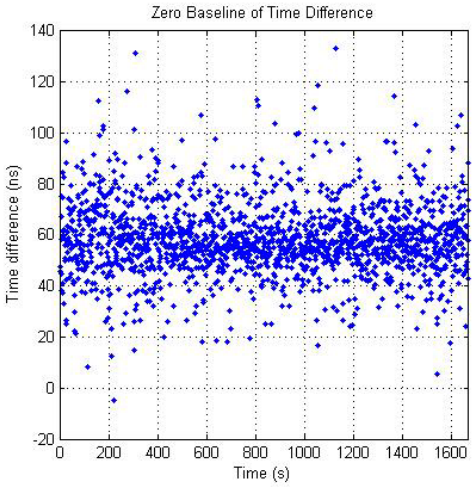

Figure 6: Time difference result for the zero baseline test with the Rubidium clock.

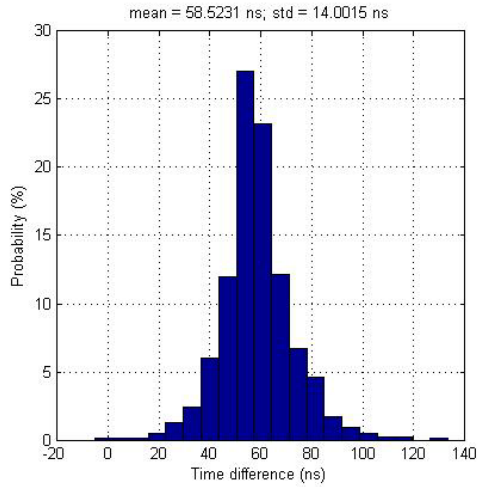

Figure 7: Histogram of time difference estimates for the Rubidium clock.

3. 1090 ADS-B WAM TEST BED FOR RANGING ASSESSMENT

The 1090 ADS-B message contains no information about the signal transmitting time (i.e., time of transmission (TOT), and the DTOA method is therefore used to assess the performance of ranging measurements. Figure 8 illustrates that the signal transmitting time information (i.e., TOT) can be eliminated by differencing TOAs from two different ADS-B ground stations as follows,

$$DTOA = TOA_2 - TOA_1 \quad (5)$$

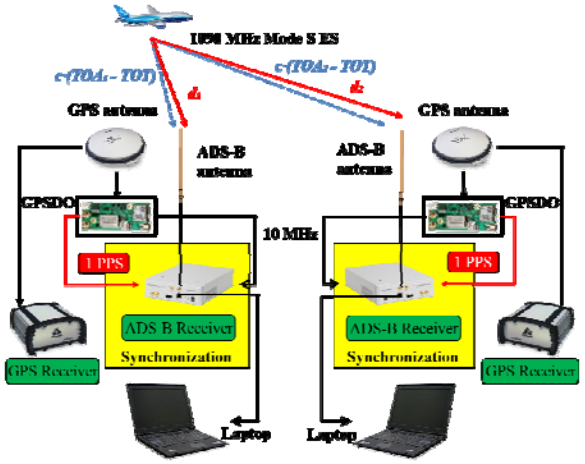

Figure 8: System configuration for the two ADS-B ground stations test.

Each of the two ADS-B ground stations records the arrival time of 1090 ADS-B signal and then obtains the traveling distance of signal by multiplying the arrival time with the speed of light. The differential ranging measurement can be calculated by the DTOA method. Also, the true differential range Δd can be obtained by differencing the true distances between the target aircraft's position and two ADS-B ground stations' positions.

$$\Delta d = d_2 - d_1 \tag{6}$$

where d_1 and d_2 are the true distances that can be calculated with the known surveyed ADS-B ground stations' positions and the aircraft's reported position from its 1090 ADS-B message. Comparing to the true differential distance obtained in Equation (6), there are several possible error sources to the DTOA measurement calculated by Equation (5), including the synchronization error, signal noise and processing error, and the error due to the bandwidth limitations on 1090 Mode S ES [9]. In order to investigate these errors, the differential range error can be calculated by differencing the estimated differential range measurement obtained from equation (5) and the true differential distance as follows:

$$Error = c \cdot DTOA - \Delta d \tag{7}$$

where c is the speed of light.

As shown in Figure 9, a two-station WAM test bed is developed for the ranging assessments around NCKU campus. The two ADS-B ground stations are time synchronized and separated by a distance of 950 meters.

Figure 9: Experimental environment for ranging assessment test.

Two example results are presented here. The nominal example result (Example I) is shown in Figures 10 and 11. Figure 10 shows several aircraft ground tracks that are obtained from the 1090 ADS-B data, and Figure 11 shows the histogram of the differential range errors of three aircraft. This aircraft use the following International Civil Aviation Organization (ICAO) addresses: 4735856, 9015459 and 9015491. For Example I, the mean of the differential range error is -9.78 m and the standard deviation is 30.68 m. As shown in Figure 12, Example I presents the nominal case that has no significant change in the recorded DTOA measurements.

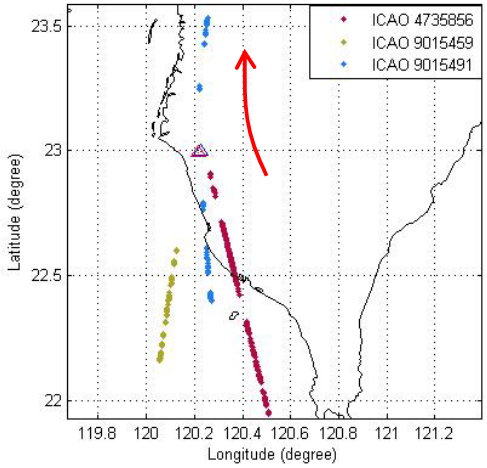

Figure 10: Example I: aircraft ground tracks obtained from 1090 ADS-B data.

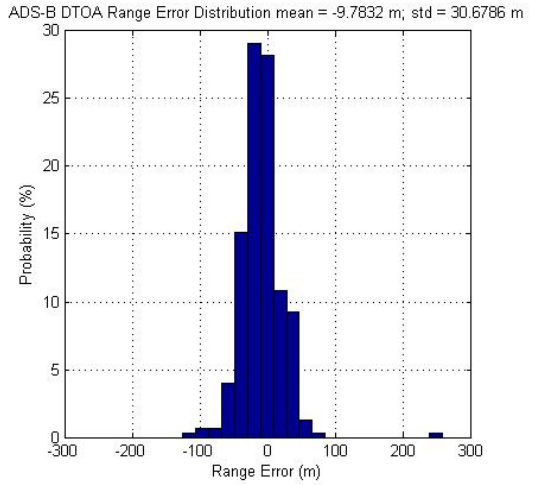

Figure 11: Example I: the histogram of the differential range errors for ICAO 4735856, 9015459 and 9015491.

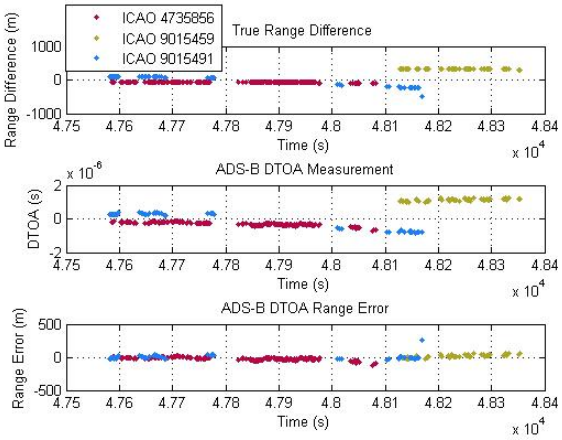

Figure 12: Example I: the true differential ranges (top), the DTOA measurements (middle) and the differential range errors (bottom).

On the other hand, Example II depicts the irregular case which has some large changes in the recorded DTOA measurements. Figure 13 shows the aircraft ground tracks obtained from the recorded ADS-B data. The histogram of the differential range errors for aircraft with ICAO addresses 7455321, 7668536 and 9015553 is shown in Figure 14. The mean differential range error of Example II is 23.85 m, and the standard deviation is 147.66 m which is larger than that of Example I. When inspecting the detailed results presented in Figure 15, one could note that there are large changes in the differential range errors for ICAO 9015553, as shown in the red box. The flight direction of ICAO 901553 is toward the two ADS-B ground stations. When aircraft is near the two stations, the quality of the time synchronization would be the dominant factor in the DTOA measurements. Specifically, in the top plot of Figure 15, the true differential range of ICAO 901553 is decreasing for the period shown in the red box. However, in the red box of the middle plot, the DTOA measurement of the same aircraft does not have the same variations. Consequently, the large differential range error is shown in the red box of the bottom plot. In addition, the received 1090 ADS-B signal strength of ICAO 901553 at the two ADS-B ground stations is shown in Figure 16. As it can be seen in the figure, the received ADS-B signal strength at Site 2 increases as the aircraft flies toward Site 2, but at the same time the received ADS-B signal strength at Site 1 remains constant even when the same aircraft closes to Site 1. This raises some issues that might be due to 1) the long coaxial cable used at Site 1, and 2) the environmental multipath effects.

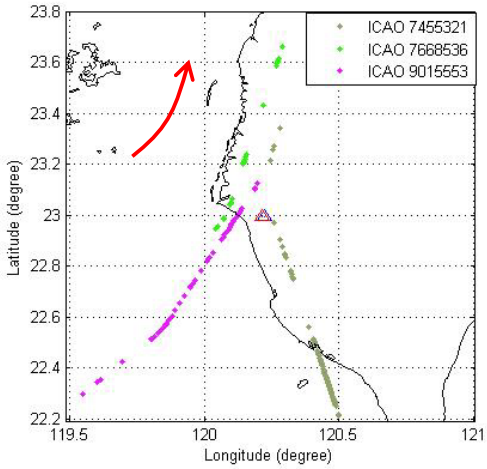

Figure 13: Example II: aircraft ground tracks obtained from 1090 ADS-B data.

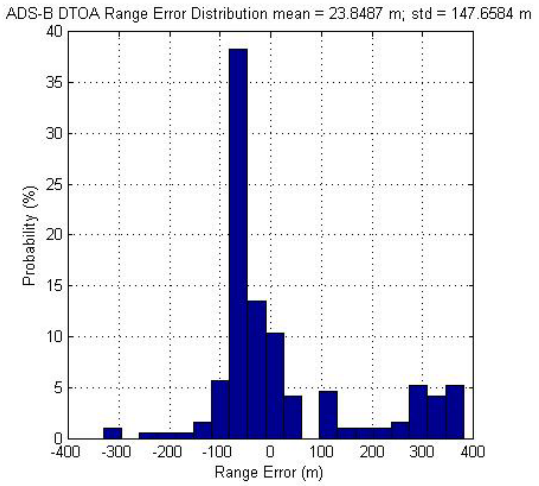

Figure 14: Example II: the histogram of the differential range errors for ICAO 7455321, 7668536 and 9015553.

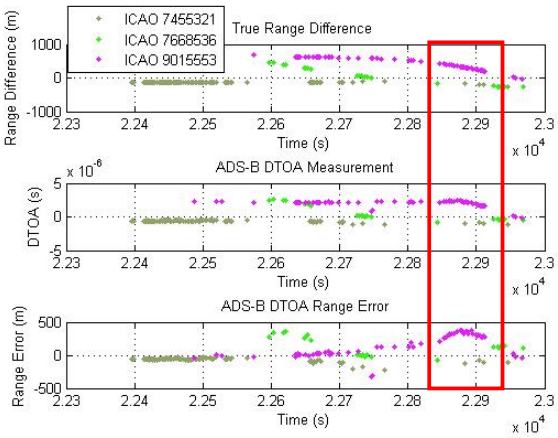

Figure 15: Example II: the true differential ranges (top), the DTOA measurements (middle) and the differential range errors (bottom).

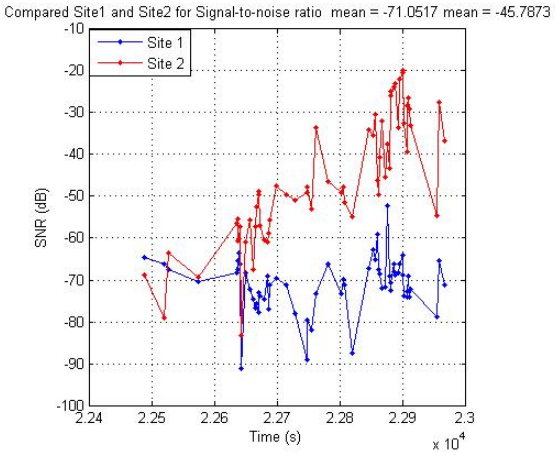

Figure 16: The received 1090 ADS-B signal strength of ICAO 9015553 at the two ground stations.

4. POSITIONING ALGORITHMS AND DILUTION OF PRECISION

As mentioned in the previous section, without the transmission timing information, the DTOA method is therefore used to provide the passive ranging measurement. According to [10], the emitter location could be estimated from a set of hyperbolic curves by the DTOA measurements. Thus, two positioning algorithms are discussed in this section, and they are 1) the linear iterative least squares method and 2) the non-iterative quadratic equation solution method. In order to gain the possible improvement on positioning performance, we propose a new positioning algorithm that combines the above two positioning algorithms. Additionally, the impact of the geometry of the ADS-B ground station distribution on positioning performance is investigated in this section.

A) Positioning algorithms

1) The linear iterative least squares method

The first positioning algorithm discussed is the linear iterative least squares method, and the widely used method to linearize a set of nonlinear equations and to obtain the precise position estimate at reasonable noise levels is the Taylor-series method [11]. As depicted in Equation (5), The DTOA range measurement can be determined by differencing the TOA range measurements obtained from several ground stations. For instance, taking the differences between all TOA range measurements (TOA_i) and that of the first ground station (TOA_1) as

$$\begin{aligned} R_{i,1} &= c\cdot\left(TOA_i - TOA_1\right) \\ &= R_i - R_1 \\ &= \sqrt{\left(x-X_i\right)^2+\left(y-Y_i\right)^2+\left(z-Z_i\right)^2} \\ &\quad -\sqrt{\left(x-X_1\right)^2+\left(y-Y_1\right)^2+\left(z-Z_1\right)^2} \end{aligned} \tag{8}$$

where R_i is true range calculated by the position of target aircraft (x, y, z) and the known surveyed location of the i^{th} ADS-B ground station (X_i, Y_i, Z_i).

The interest of this paper is to provide the horizontal positioning service. When the positioning algorithm is used to solve the Equation (8), the vertical position of the target aircraft uses the barometric altimeter reading reported in the ADS-B message, and then the positioning algorithm is used to solve the two unknowns (East, North) in the horizontal position. Also, the vertical position information gained from the ADS-B message has to be transferred to the coordinate system of the positioning algorithm used in this paper, the earth-centered earth-fixed (ECEF) coordinate frame [13].

In the Taylor-series method, we first linearize the Equation (8) by Taylor-series expansion and then give an initial position guess $(\hat{x}, \hat{y}, \hat{z})$ to solve it iteratively by the least squares method [11]. The position solution is converged when $(\Delta x, \Delta y, \Delta z)$ are sufficiently small [12]. The calculation can be expressed as follows,

$$\begin{bmatrix}\Delta x\\ \Delta y\\ \Delta z\end{bmatrix} = \left(H^T H\right)^{-1} H^T h \tag{9}$$

where

$$h = \begin{bmatrix} R_{2,1} - \left(\hat{R}_2 - \hat{R}_1\right) \\ R_{3,1} - \left(\hat{R}_3 - \hat{R}_1\right) \\ \vdots \\ R_{M,1} - \left(\hat{R}_M - \hat{R}_1\right) \end{bmatrix} \tag{10}$$

$$H=\begin{bmatrix} \frac{(X_1-\hat{x})}{R_1}-\frac{(X_2-\hat{x})}{R_2} & \frac{(Y_1-\hat{y})}{R_1}-\frac{(Y_2-\hat{y})}{R_2} & \frac{(Z_1-\hat{z})}{R_1}-\frac{(z_2-\hat{z})}{R_2} \\ \vdots & \vdots & \vdots \\ \frac{(X_1-x)}{R_1}-\frac{(X_i-\hat{x})}{R_i} & \frac{(Y_1-\hat{y})}{R_1}-\frac{(Y_i-\hat{y})}{R_i} & \frac{(Z_1-\hat{z})}{R_1}-\frac{(Z_i-\hat{z})}{R_i} \end{bmatrix} \quad (11)$$

The symbol of $R_{i,1}$ is calculated by Equation (8). The symbol of $\hat{R}_i$ is a estimated range by the initial guess $(\hat{x},\hat{y},\hat{z})$. For this linear iterative least squares method, there are two issues that need to be considered in the implementation of this method in the ADS-B WAM: 1) the initial position guess of aircraft, and 2) the convergence of the position solution. Therefore, another positioning algorithm, the non-iterative quadratic equation solution method is used in this test bed to avoid above issues.

2) The non-iterative quadratic equation solution method

There is another method to solve Equation (8) proposed by Chan in [14]. Chan's method gave a closed form approximation of the maximum likelihood (ML) estimator when DTOA estimation errors are small [14]. Again, the goal of this paper is to provide horizontal positioning service. Therefore, for testing this positioning algorithm, we use the vertical position obtained from the ADS-B message, and then transform the vertical position to be in the same coordinate frame used in Chan's method. The local East-North-Up (ENU) frame is used here, so the target aircraft position (x,y,z) and the ADS-B ground station position (X_i,Y_i,Z_i) need to be transformed to (e,n,u) and (E_i,N_i,U_i), respectively. Then, we calculate the DTOA difference, $\Delta DTOA_{ENU}$, in ENU frame using the known aircraft position derived from ADS-B message and the known surveyed station position. Next, we sum this $\Delta DTOA_{ENU}$ term with the estimated $DTOA_{i,1}$ in meters to form the horizontal DTOA measurement (i.e., $DTOA_{i,1,EN}$) as follows,

$$DTOA_{i,1,EN}=c\cdot(TOA_i-TOA_1)_{estimated}+\Delta DTOA_{ENU} \quad (12)$$

Write Equation (8) as $R_i^2=(R_{i,1}+R_1)^2$ and it then can be rewritten in ENU frame as

$$R_{i,1}{}^2+2R_{i,1}R_1=K_i-2eE_{i,1}-2nN_{i,1}+K_1 \quad (13)$$

where

$$R_1=\sqrt{(e-E_1)^2+(n-N_1)^2} \quad (14)$$

The symbols $E_{i,1}$ and $N_{i,1}$ are E_i-E_1 and N_i-N_1, respectively. The symbols K_i and K_1 stand for $E_i^2+N_i^2$ and $E_1^2+N_1^2$, respectively.

With three ADS-B ground stations, the positioning solution of (e,n) can be written in terms of R_1 as

$$\begin{bmatrix} e \\ n \end{bmatrix}=-\begin{bmatrix} E_{2,1} & N_{2,1} \\ E_{3,1} & N_{3,1} \end{bmatrix}^{-1}\times\left\{\begin{bmatrix} DTOA_{2,1,EN} \\ DTOA_{3,1,EN} \end{bmatrix}R_1+\frac{1}{2}\begin{bmatrix} DTOA_{2,1,EN}{}^2-K_2+K_1 \\ DTOA_{3,1,EN}{}^2-K_3+K_1 \end{bmatrix}\right\} \quad (15)$$

Insert Equation (15) back into Equation (14) to form a quadratic equation in terms of R_1. This quadratic equation has two roots that lead to two possible solutions. The solution R_1 can be resolved by restricting the transmitter to be in the region of interest, and then plug this back into the Equation (15) to obtain the final position solution. As is shown later, the positioning performance of this non-iterative quadratic equation solution method (Chan's method) is less accurate than that of the linear iterative least squares method (Taylor-series method), but Chan's method does not have any divergence issue. However, Chan's method gives multiple possible correct solutions. In order to gain better positioning accuracy and solution availability, the new positioning algorithm that combines the Chan's method and the Taylor-series method is proposed in this work.

3) The hybrid method of Chan's method and Taylor-series method

The above mentioned positioning algorithms have their advantages and disadvantages in different aspects. Therefore, it is possible to get better positioning performance if the two positioning algorithms could be combined in a complementary way. That is, the hybrid positioning algorithm uses Taylor-series method as the default, because Taylor-series method gives positioning solution with better accuracy if the iterations are converged. Moreover, the initial position guess to the Taylor-series method is the key factor in the solution convergence. If Taylor-series method cannot provide a converged position solution, then, in this proposed hybrid method, we will first use the previous aircraft position and velocity information obtained from the ADS-B message (before losing GPS signal) to select the reasonable position solution from Chan's method, and this position solution is used as the initial guess to run the Taylor-series method. The procedure of the proposed positioning algorithm is summarized in Figure 17.

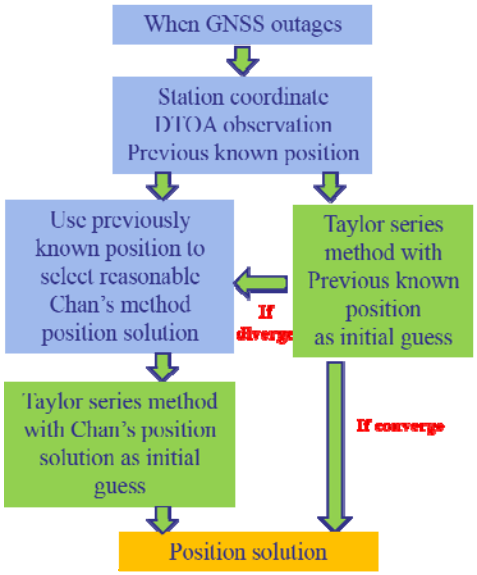

Figure 17: The positioning procedure of the combined use of Taylor-series method and Chan's method.

B) Dilution of precision

The additional factor that affects the positioning performance of the developed 1090 ADS-B WAM test bed is the geometry of the ground station distribution and thus called the dilution of precision (DOP). The definition of the DOP for our 1090 ADS-B WAM test bed is as follows [15],

$$DOP = \frac{\sigma_p}{\sigma_r} = \sqrt{trace\left(H^T H\right)^{-1}} \tag{16}$$

where σ_p is the position error; σ_r is the range error, and H is the DTOA observation matrix defined in Equation (11).

The positional DOP (PDOP), horizontal DOP (HDOP) and vertical DOP (VDOP) are represented respectively as [16]

$$PDOP = \sqrt{\left[(H^T H)\right]_{1,1} + \left[(H^T H)\right]_{2,2} + \left[(H^T H)\right]_{3,3}} \tag{17}$$

$$HDOP = \sqrt{\left[(H^T H)\right]_{1,1} + \left[(H^T H)\right]_{2,2}} \tag{18}$$

$$VDOP = \sqrt{\left[(H^T H)\right]_{3,3}} \tag{19}$$

The HDOP is the interest of this paper; as shown later in this paper, the value of HDOP less than 5 is needed to meet the surveillance requirement of APNT.

5. EXPERIMENTS AND RESULTS

In order to evaluate the positioning performance of three different positioning algorithms described in the previous section, three 1090 ADS-B ground stations are installed around NCKU campus to form a WAM test bed, and the geographical distribution of the ground stations is illustrated in Figure 18.

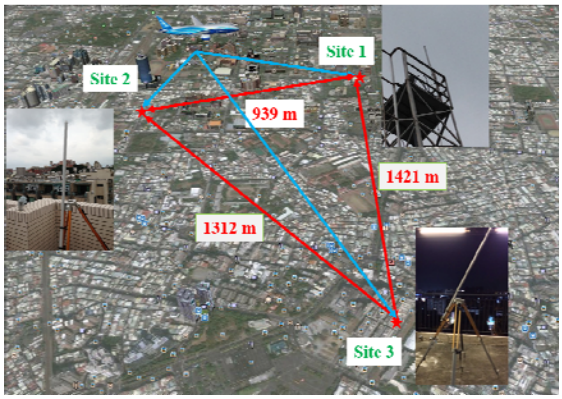

Figure 18: Arrangement of three ADS_B ground stations for the positioning test.

Figure 19 shows the positioning results for ICAO 4735856. In the figure, three triangles represent the locations of three ADS-B ground stations. The blue dots indicate the true position of the aircraft derived from ADS-B message. The red diamonds represent the positioning result by the Taylor-series method, the green squares are the positioning result using the Chan's method, and the purple circles are the positioning result using the proposed hybrid method. The comparison plots of positioning results in East and North directions using Taylor-series method and Chan's method are shown in Figure 20. The mean and standard deviation of the positioning results are summarized in Table 1. One could observe form the figure that Taylor-series method outperforms Chan's method in terms of positioning accuracy. As noted before, Taylor-series method may fail to converge due to poor initial position guess or the poor geometry of the ground station (i.e., large HDOP) or both. The Chan's method has relatively poorer positioning accuracy but no convergence issue. Therefore, this paper proposes a new positioning method to combine the above two methods. The horizontal positioning results are shown in Figure 21, and the mean and standard deviation of the positioning results are depicted in Table 2. The combined use of Taylor-series method and Chan's method gives better positioning performance than that of the two methods alone with respect to the mean of positioning error. Additionally, the hybrid method yields more converged position solution than that of the original Taylor-series method.

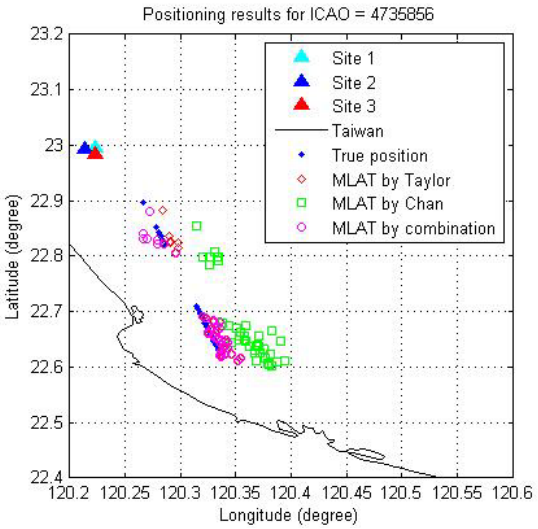

Figure 19: ICAO 4735856 positioning results using three positioning algorithms.

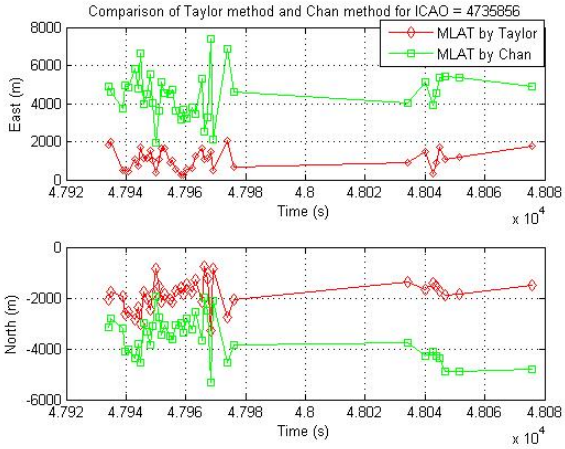

Figure 20: The East (top) and North (bottom) positioning errors for Taylor-series method (red) and Chan method (green).

Table 1: The East and North positioning errors for Taylor-series method and Chan method.

Taylor Position Error (m)			
East μ	**North μ**	**East σ**	**North σ**
1068.27	-1887.53	519.71	567.89
Chan Position Error (m)			
4475.47	-3559.1	1177.53	837.11

Table 2: The East and North positioning errors for the hybrid method.

The Hybrid Method Position Error (m)			
East μ	**North μ**	**East σ**	**North σ**
754.01	-1806.09	841.34	634.58

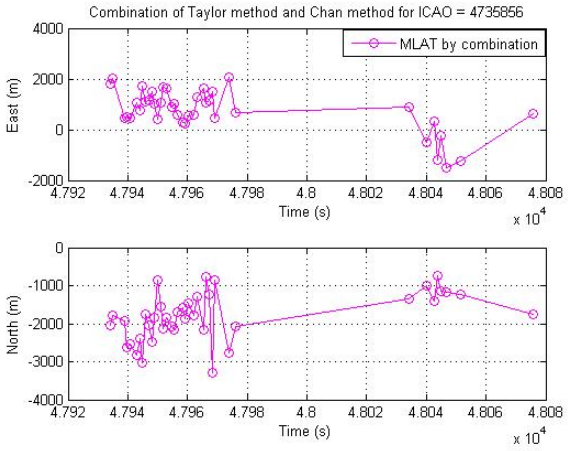

Figure 21: The East (top) and North (bottom) positioning errors for the hybrid method.

The top plot of Figure 22 shows the horizontal position error; the middle plot indicates the corresponding HDOP values, and the aircraft altitude obtained from ADS-B message is shown in the bottom plot. Then, we calculate the equivalent range error using the relationship shown in Equation (16), that is, the horizontal position error divided by the corresponding HDOP, and the results are shown in Figure 23. The mean of the equivalent range error is about 18.7 m which is very similar to the range error (21.77 m) found in the range assessment test as shown in Figure 24. Namely, the ranging accuracy is close to the current surveillance target for 3 mile separation (≤ 32.7 m, 2 standard deviation) [4]. However, the large positioning errors are mainly due to the large HDOP values (about 100) shown in Figure 22. Similar results were presented in [1].

In order to investigate the impact of HDOP on the positioning performance of the ADS-B WAM test bed, three simulations are conducted in this work:

1) Current three 1090 ADS-B ground stations with good ranging accuracy shown in Section 3 (i.e., $\mu = -9$ m and $\sigma = 30$ m).
2) Current three 1090 ADS-B ground stations with inadequate ranging accuracy shown in Section 3 (i.e., $\mu = 23$ m and $\sigma = 147$ m).
3) Extended three 1090 ADS-B ground stations with good ranging accuracy shown in Section 3 (i.e., $\mu = -9$ m and $\sigma = 30$ m).

The positioning algorithm used in the simulations is the Taylor-series method, and the aircraft altitude is 30,000 ft. Figure 25 shows the simulation result for the first case. In the figure, the red regions are of positioning errors larger than 5,000 m, and the blue region are of positioning errors less than 500 m. One notes that the regions close to the ground stations have better positioning performance, because the geometry diversity is better for aircraft approaching the ground stations (i.e., smaller HDOP values). The second simulation result is shown in Figure 26. As expected, most regions have positioning error larger than 5,000 m (in red). For the third simulation, we

extend the locations of three ADS-B ground stations are placed at the Taiwan coastline with good separation as shown in Figure 27 (Note: the color bar scale (0~100 m) of Figure 27 is different than that of Figures 25 and 26 (0~5,000 m)). In the figure, most of regions have positioning error less than 50 m which is close to the surveillance requirement of APNT (92.6 m, 2 standard deviation) [4], and these regions are all have HDOP values less than 5.

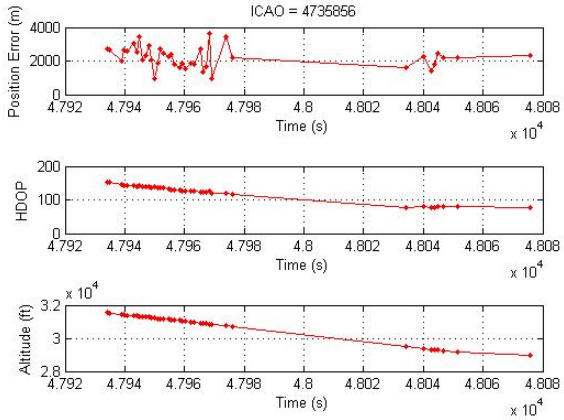

Figure 22: ICAO 4735856 horizontal position error (top), HDOP values (middle) and the corresponding aircraft altitude (bottom).

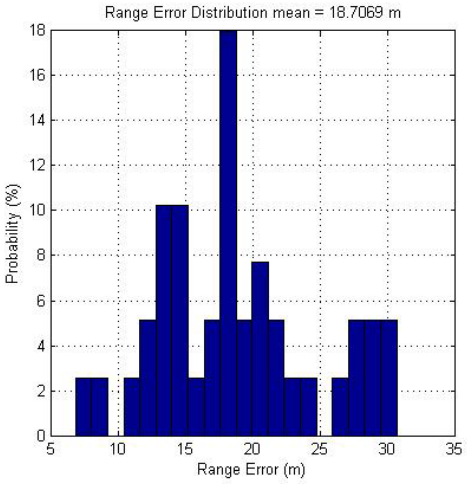

Figure 23: ICAO 4735856 equivalent ranging error in the positioning assessment test.

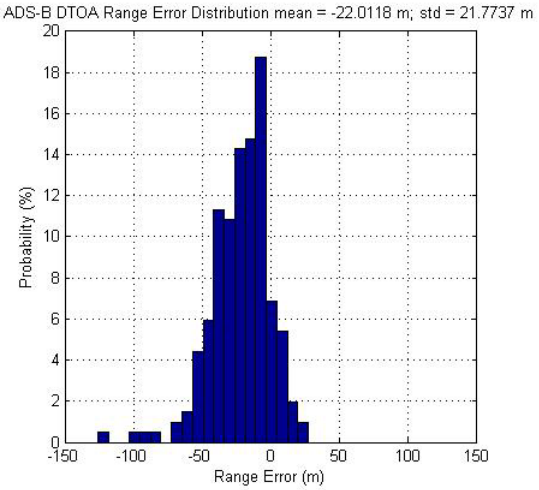

Figure 24: ICAO 4735856 ranging error in the ranging assessment test.

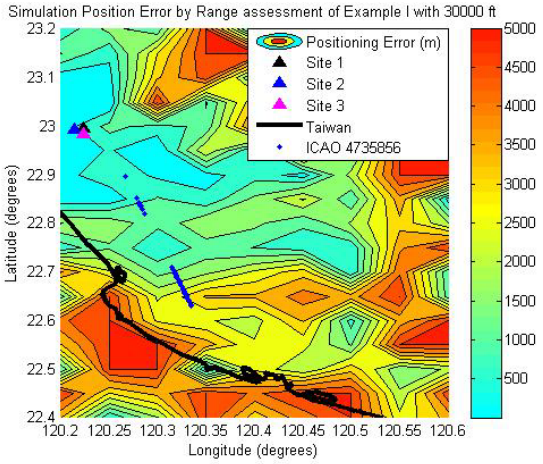

Figure 25: Positioning error simulation result for the current three 1090 ADS-B ground stations with ranging accuracy of $\mu = -9$ m and $\sigma = 30$ m.

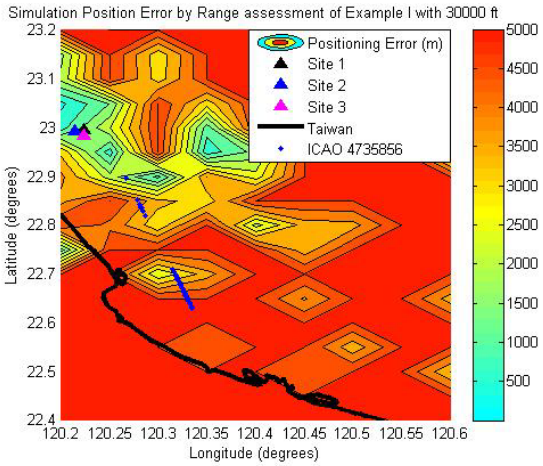

Figure 26: Positioning error simulation result for the current three 1090 ADS-B ground stations with ranging accuracy of $\mu = 23$ m and $\sigma = 147$ m.

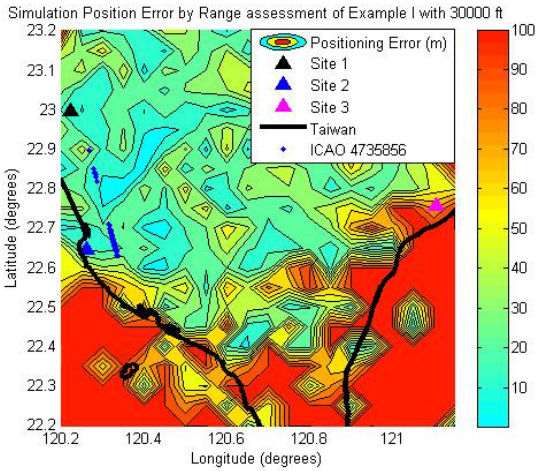

Figure 27: Positioning error simulation for the extended three 1090 ADS-B ground stations with ranging accuracy of $\mu = -9$ m and $\sigma = 30$ m (Note: the color bar is in different scale than that of Figures 25 and 26).

6. CONCLUSION AND FUTURE WORK

In this work, we developed a wide area multilateration (WAM) test bed using 1090 MHz ADS-B signal to evaluate its positioning performance as an alternative position navigation and timing (APNT) system. We used all commercial off the shelf (COTS) components, USRP and GPSDO, to build each ADS-B ground station. In addition, for a multilateration system, there were three important factors to the positioning performance: 1) timing measurement, 2) range measurement, and 3) geometry distribution of ground stations. Therefore, we conducted a zero baseline experiment to validate our synchronization scheme. As shown in the experiment results, with the cross-correlation and interpolation techniques, the developed ADS-B ground stations were synchronized with accuracy of 13 ns (2 standard deviations) which was well below the surveillance requirement of APNT (50 ns). In other words, the developed synchronization scheme of our test bed was sufficient. We then developed a two-station experiment to investigate the passive ranging performance, and as indicated in the experiment results, the standard deviation of the differential range errors was about 30 m under nominal conditions which also met the surveillance requirement of APNT (32.7 m). However, there were some irregular cases showing the standard deviation of the differential range errors around 150 m for the same two-station setup. As shown in the paper, the large differential ranging error might be caused by the long coaxial cable used in test equipment or local environmental effects (e.g., multipath). For the actual positioning performance, we used a three-station test bed to evaluate three positioning algorithms, and they are 1) Taylor-series method, 2) Chan's method, and 3) the hybrid of 1) and 2). Based on the experiment results, Taylor-series method outperformed Chan's method in terms of positioning accuracy. However, Taylor-series method did suffer from the divergence issues, and Chan's method gave multiple possible correct solutions. As a result, the hybrid method of prior two methods was proposed in this paper to improve positioning performance. As shown in the experiment results, the hybrid method gave more position fixes and more accurate fixes. Importantly, this is beneficial in situations with large horizontal dilution of precision (HDOP). Currently, the HDOP was the dominant factor to meet the APNT requirement. Therefore, three simulations were conducted in this work to seek the appropriate HDOP values for such an ADS-B WAM test bed to support APNT. As demonstrated in the simulation results, HDOP of 5 or less was needed to meet surveillance requirement of APNT.

Our next step is to continue this 1090 ADS-B WAM test bed with additional ground stations separated with extended distances to assess the DTOA positioning performance. Additionally, the maximum aircraft capacity problem and the downlink data collision problem for a ground ADS-B SDR receiver have to be studied in the future.

ACKNOWLEDGMENTS

The work presented in this paper is supported by Taiwan Ministry of Science and Technology under project grant: NSC 101 – 2628 – E – 006 – 013 – MY3. The authors gratefully acknowledge the support.

REFERENCES

[1]. Chen, Y-H., Lo, S., Akos, D.M., Wong, G., Enge, P., *"A Testbed for Studying Automatic Dependent Surveillance Broadcast (ADS-B) Based Range and Positioning Performance to Support Alternative Position Navigation and Timing (APNT),"* Proceedings of ION GNSS+ 2013, Nashville, TN, September 2013, pp. 263-273. Federal Aviation Administration, NextGen Implementation Plan, March 2012.

[2]. Jan, S-S., Jheng, S-L., Tao, A-L., *"Wide Area Multilateration Evaluation Test Bed using USRP Based ADS-B Receiver,"* Proceedings of ION GNSS+ 2013, Nashville, TN, September 2013, pp. 274-281.

[3]. Chen, Y-H., Lo, S., Akos, D.M., De Lorenzo, D., Enge, P., *"Validation of a Controlled Reception Pattern Antenna (CRPA) Receiver Built from Inexpensive General-purpose Elements During Several Live Jamming Test Campaigns,"* Proceedings of the Institute of Navigation ITM Conference, San Diego, CA, January 2013

[4]. Lo, S., *"Pseudolite Alternatives for Alternate Positioning, Navigation, and Timing (APNT),"* FAA White Paper, August 2012, reachable on the web at http://www.faa.gov/.

[5]. Lo, S., Akos, D.M., Dennis, J., "*Time Source Options for Alternate Positioning Navigation and Timing (APNT)*, White Paper, August 2012.
[6]. Kim, E., *Investigation of APNT Optimized DME/DME Network Using Current State-of-the-Art DMEs*, IEEE/ION PLANS 2012.
[7]. Jacovitti, G., Scarano, G., *"Discrete time techniques for time delay estimation,"* Signal Processing, IEEE Transactions on, Feb 1993, pp. 525-533.
[8]. Narins, M., Enge, P., Peterson, B., Lo, S., Chen, Y.-H., Akos, D.M., Lombardi, M., *"The Need for a Robust Precise Time and Frequency Alternative to Global Navigation Satellite Systems,"* Proceedings of ION GNSS 2012, Nashville, TN, September 2012, pp. 2057-2062.
[9]. RTCA DO-260A, *"Minimum operational performance standards for 1090 MHz Extended Squitter Automatic Dependent Surveillance-Broadcast (ADS-B) and Traffic Information Services-Broadcast (TIS-B),"* 2003.4.10.
[10]. Rappaport, T.S. Reed, J.H., Woerner, B.D., *"Position Location Using Wireless Communications on Highways of the Future,"* IEEE Communications Magazine, October 1996.
[11]. Foy, W.H., *"Position-location solutions by Taylor-series estimation,"* IEEE Trans. Aerosp. Electron. Syst., vol. AES-12, pp. 187-194, Mar. 1976.
[12]. Tonieri, D.J., *"Statistical theory of passive location systems,"* IEEE Trans. Aerosp. Electron. Syst., vol. AES-20, pp. 183-198, Mar. 1984.
[13]. Misra, P., Enge, P., *"Global Positioning System: Signals, Measurement, and Performance,"* 2nd Edition, Ganga-Jamuna Press, Lincoln, MA., 2006.
[14]. Chan, Y.T., A Simple and Efficient Estimator for Hyperbolic Location, IEEE Transactions on Signal Processing, 1994.
[15]. Pei, X., Huang, Z., Zhu, Y., Liu, W., "Research on the relationship between DOP and the number of stations for multilateration system," 2010 IEEE International Conference on Information Theory and Information Security, 2010.
[16]. Li, B., Dempster, A.G., Wang, J., *"3D DOPs for Positioning Applications Using Range Measurements,"* Wireless Sensor Network, vol. 3, no.10, pp. 334-340, 2011.